# Journal of Materials Chemistry B

Accepted Manuscript






ROYAL SOCIETY OF CHEMISTRY

www.rsc.org/materialsB

Cite this: DOI: 10.1039/c0xx00000x

www.rsc.org/xxxxxx

ARTICLE TYPE

# Tunable functionality and nanogeometry in tetrahydrofuran hydroperoxide and 3-Aminopropyl-trimethoxysilane mediated synthesis of gold nano-particles; Functional application in Glutathione sensing

**Prem. C. Pandey and Gunjan Pandey**

***Received (in XXX, XXX) Xth XXXXXXXXX 20XX, Accepted Xth XXXXXXXXX 20XX***
**DOI: 10.1039/b000000x**

## ABSTRACT

Substantive research on controlled synthesis of noble metal nanoparticles displaying tunable functionality and nanogeometry has been a challenging requirement. We report herein a process involving the active role of tetrahydrofuran hydroperoxide (THF-HPO) and 3- aminopropyltrimethoxysilane (3-APTMS) that allow controlled synthesis of functional gold nanoparticles (AuNPs) with following major findings: (1) An increase in 3-APTMS concentrations causes increase in size whereas the same for THF-HPO shows reverse effect, (2) different size of AuNPs at same concentration of 3-APTMS can be made by controlling THF-HPO, (3)addition of 3-APTMS even after AuNPs synthesis allow control over nanogeometry, (4) formation of γ-Butyrolactone (GBL) during nanoparticle synthesis which itself participates in AuNPs synthesis. Furthermore, the functionality and nanogeometry of as synthesized AuNPs are utilized in Glutathione sensing that justified the pivotal role of functionality as compared to nanogeometry.

## INTRODUCTION

Functionalization of noble metal nanoparticles with a wide range of organic or biological ligands has received wider attention for the selective binding and detection of small molecules and biological targets.[1-4] Functionality in metal nanoparticles is important in determining its application for various practical purposes. Many reports are available where functionality has played a vital role.[5-7] In addition to that the size of these nanomaterials have remarkable influence on the binding events enabling the development of innovative technological designs.[8] Accordingly, the synthesis of nanoparticles displaying tunable functionality and nanogeometry has been a challenging requirement.

Nanomaterials functionalized/stabilized through amino group has received closer attention due to their ubiquitous nature specialy in biological and enviromental systems as such functionality enable biocompatible linkage.[9-10] In addition to that AuNPs are being tried for their use in cancer therapy as drug carriers, photothermal agents, contrast agents and radiosensitisers.[11] Organically-soluble gold nanocrystals passivated with alkylamines have shown their chemical and physical characteristics that are consistent with charge-neutral amine/gold surface interactions described by weak covalent bonds.[12] Amines form only weakly bound and chemically unstable monolayers on bulk Au surfaces. In contrast, the amine-capped nanocrystals are nearly as stable as their thiol-capped counterparts.[12] Apart from these functional activity of organic amine, large number of report display their stabilizing and reducing ability for noble metal salts.[13-16] Newman et al. reported the ability of various amine as reducing and stabilizing agent useful in the formation of AuNPs based on Marcus electron transfer theory.[17] Apart from these activity, organic amine functionalized alkoxysilane and in combination with other functional alkoxysilane silane especially 2-(3,4-epoxycyclohexyl)-ethyltrimethoxysilane has enabled the formation of controlled nanostructured biocompatible thin film of organically modified silicate.[18] Zhu et. al. have reported the synthesis of AuNPs utilizing active role of amines as capping and reducing agent having trimethoxysilane moiety. They used 3-(trimethoxysilylpropyl) diethylenetriamine (TMSP diene) for AuNPs synthesis and found that the ratio of TMSP/$Au^{3+}$ control the nanogeometry of resulting AuNPs. Time required for AuNPs formation varied from 2hrs to 23hrs depending on the ratio of TMSP/$Au^{3+}$.[19] They also observed very slow conversion to nanoparticles when 3-APTMS and trimethoxysilylpropyl ethylenediamine were used in

place of TMSP. These findings reveals the reducing and stabilizing ability of 3-APTMS however predict the requirement of additional reducing agent for rapid and controlled nanoparticle synthesis. We have already demonstrated the role of 3-GPTMS that efficiently facilitate the reduction of $Pd^{2+}$ ions[20] demonstrating the opening of epoxide ring of 3-GPTMS by lewis acid character of palladium chloride. Such functional ability of 3-APTMS and 3-GPTMS has subsequently been examined on the controlled conversion of gold nanoparticles(AuNPs), Silver nanoparticles (AgNPs) and Palladium nanoparticles (PdNPs) from respective noble metal salts where nanogeometry varied as a function of ratio of 3-APTMS/3-GPTMS at constant $Au^{3+}$ concentration[21].Apart from many functional activity, dispersibility in both aqueous and non-aqueous medium and biocompatibility of these nanoparticles, the use of two alkoxysilanes of optimum concentrations restricted to prevent the silanol group hydrolysis to form Si-O-Si linkage, hence, posing problem in use of these material for many required practical purposes. Accordingly, exchange of 3-GPTMS by other suitable biocompatible organic reagent is sought. THF-HPO[22] along with 3-APTMS has been found a better option which not only reduced the silane content but also expedited nanoparticle formation with an additional advantage of producing biocompatible reaction product. The choice of these reagents during noble metal nanoparticles synthesis enabled; (1) control of nanogeometry as a function of 3-APTMS concentration, (2) control of nanogeometry as a function of 3-APTMS concentration even after the synthesis of nanoparticles, and (3) control of nanogeometry as a function of tetrahydrofuran hydroperoxide concentration even at constant concentrations of 3-APTMS. The novel finding justifying concentration dependent tuning of functional activity and nanogeometry even after the synthesis which have been challenging requirement in the area of nanoparticle synthesis is reported in this communication.

Glutathione is a biologically important molecule and have specific interaction with hydrogen peroxide.[23] Such specific interaction has been manipulated by the use of nanomaterials for precise GSH sensing. [24-25] In addition to that GSH has also affinity for monolayer assembly on gold surface.[26] Accordingly, functional noble metal nanoparticles like AuNPs may provide valuable information on GSH sensing and the role of functionality could be manipulated based on differential catalytic ability of 3-APTMS-functionalized AuNPs and GSH activity. Fortunately, we recorded interesting finding demonstrating AuNP-dependent catalysis of O-dianisidine in the presence of $H_2O_2$ as a function of GSH concentration. The catalytic oxidation of O-dianisidine has also been found as the function of 3-APTMS concentrations of as synthesized AuNPs representing first report on the role of functional ability of AuNPs in chemical sensing. In addition to that a comparison on the catalytic efficiency of AuNPs in GSH sensing as a function of functionality and nanogeometry have also been demonstrated.

## EXPERIMENTAL SECTION

### Chemicals

The following chemicals were used: 3-aminopropyltrimethoxysilane (3-APTMS) was obtained from Aldrich Chem. Co.; Tetrachloroauric acid, were purchased from HiMedia; hydrogen peroxide, glutathione were obtained from Merck, India. O-dianisidine was obtained from Loba Chemie. All other chemicals employed were of analytical grade. Aqueous solutions were prepared by using doubly distilled-deionized water (Alga water purification system).

### Synthesis of functional AuNPs.

### 3-APTMS and THF-HPO mediated AuNP synthesis

The typical process for AuNPs synthesis involves the mixing of an aqueous solution of metal salts and 3-APTMS at a desired ratio (Table 1). The 3-APTMS treated metal salt was then allowed to interact with THF-HPO. Synthesis of AuNPs was observed under following two conditions: (1) Varying 3-APTMS (Table 1, sample no. i-vi) at constant concentration of THF-HPO and (ii) Varying THF-HPO (Table 1, sample no. vii-xiii, iv, vi) and keeping the concentration of 3-APTMS constant. A typical THF-HPO and 3-APTMS mediated synthesis of AuNPs sol was conducted as follows: 50µl of 10mM of $HAuCl_4$ solution in water was premixed with 40 µL aqueous solution of 3-APTMS stirred for 2 minutes, followed by addition of THF-HPO. The volume was made up to 2ml with water in each case. The solution was kept undisturbed in dark for 30 minutes. AuNPs sols of red/purple/blue color were obtained within <30 min indicating the formation of different size of AuNPs.

### 3-APTMS and GBL mediated synthesis of AuNPs

50µl of 10mM of HAuCl4 solution in water was premixed with varying concentrations of 40 µL aqueous solution of 3-APTMS (Sample No. xiv-xvi, Table 2) stirred for 2 minutes, followed by addition of varying GBL concentration (Sample No. xvii-xix, Table 2)..The volume was made up to 130µl in each

case.The solution was kept undisturbed in dark for 3-4 hours.

**Peroxidase-like Catalytic Activity of AuNPs synthesized**

The peroxidase like activity of as synthesized AuNPs was determined spectrophotometrically by measuring the formation of oxidized product of o-dianisidine at 430 nm ($\varepsilon$ = 11.3 $mM^{-1}cm^{-1}$) using a Hitachi U-2900 spectrophotometer. Typically, the o-dianisidine oxidation activity was measured in water using o-dianisidine at 25°C. In brief, 40µL of 3.2M H2O2, 70µl of 10mM o-dianisidine , and 200µl of AuNPs were added into 500.0 µL of water and then the solution was mixed up to make it uniform and spectra for the three shades was recorded at fixed time intervals.

**GSH detection by measuring the wastage of H2O2**

The GSH samples were detected according to the following steps: 40µL of 3.2M $H_2O_2$, 25µl of different concentrations of GSH, 70µL of 10mM o-dianisidine and 200µL of synthesized AuNPs were added into 500 µL of water. After incubating for 75 min, the measurement was started .The absorbance change was monitored at 430nm .The final concentrations of GSH in the system varied from 24.5µM to172µM.

**Kinetic Parameters Analysis.**

The steady-state kinetics were performed by varying the concentration of H2O2 (58.9mM-980µM), at fixed concentration of o-dianisidine(344.0µM). The reaction was carried out in 2 ml water and the variation of absorbance was monitored using a spectrophotometer (Hitachi U-2900) in time scan mode at 430 nm ($\varepsilon$ = 11.3 $mM^{-1}cm^{-1}$). The kinetic parameters were calculated by fitting the absorbance data to Michaelis-Menten equation as,

$$\nu = Vmax[C] / Km + [C]$$

Where $\nu$ is the initial velocity, Vmax is the maximal reaction velocity, C is the concentration of the substrate, and Km is the Michaelis-Menten constant.

## RESULTS AND DISCUSSION

3-APTMS and THF-HPO mediated synthesis of AuNPs. We have recently reported 3-APTMS and 3-GPTMS mediated synthesis of noble metal nanoparticles (AuNPs, AgNPs and PdNPs) which are dispersible in both aqueous and non-aqueous medium simply by varying the constituents ratio.[21,27] Such findings although provided novel report on the synthesis of biocompatible noble metal nanoparticles, but suffers a disadvantage due to increased alkoxysilane content which limits its use for many practical applications due to formation of Si-O-Si linkage with time. Accordingly we tried to decrease the silane content by substituting some other reagent in place of alkoxysilanes. Since, 3-APTMS acts not only as reducer but also as a potential stabilizer[28-30], we preferred for potential substitute of 3-GPTMS. Fortunately, the choice of THF-HPO provided valuable information on the synthesis that not only decreased the silane content but also expedited the controlled formation AuNPs, PdNPs and mixed Pd-AuNPs. THF-HPO used was readily available by the autooxidation of Tetrahydrofuran.[31] The detail investigation on the synthesis of AuNPs is discussed herein.

At first instance we investigated the role of 3-APTMS and THF-HPO in reducing $Au^{3+}$ and creating the stabilized nanoparticles. It has been found that the concentration-dependent participation of both 3-APTMS and THF-HPO are necessary for converting $Au^{3+}$ ions into AuNPs of desired nanogeometry. It has also been found that 3-APTMS capped $Au^{3+}$ ions undergo rapid nanoparticles synthesis as described earlier.[21] Accordingly, the conversion of constant concentration of chloroauricacid solution (0.25mM) into AuNPs are examined under two different conditions: (i) Varying 3-APTMS while keeping THF-HPO concentration constant (fig.1), and (ii) varying the THF-HPO (Fig. 2 A, B, C) concentration while keeping 3-APTMS constant. In a typical experiment THF-HPO (11.3 mg) is added to the amino capped $Au^{3+}$ as shown in table-1. An increase in $\lambda_{max}$ with increasing 3-APTMS concentration (Table-1, system i-vi) and reverse for increasing THF-HPO (Table-1, system vii-xiii, iv, vi) was confirmed from the spectrophotometric analysis of the nanoparticles as shown in Fig.1 and Fig.2 respectively. There is a well established relationship between AuNP size and plasmon band position, with the plasmon resonance band shifting to the red and broadening with increasing particle size[32]. Thus, data shown in table-1 on $\lambda_{max}$ data demonstrate that an increase in 3-APTMS concentration results into increase in size of AuNPs, however, the same decreases on increasing the THF-HPO content (Table 1(vii-ix, x-xi and xii-xiii). These findings predict the possibility of perfect control of nanogeometry based on fixed ratio of 3-APTMS/THF-HPO. This flexibility in synthetic route to get lower nanogeometry of AuNPs even at high 3-APTMS concentration by addition of THF-HPO and higher nanogeometry nanoparticles by increasing 3-APTMS at constant concentration of THF-HPO

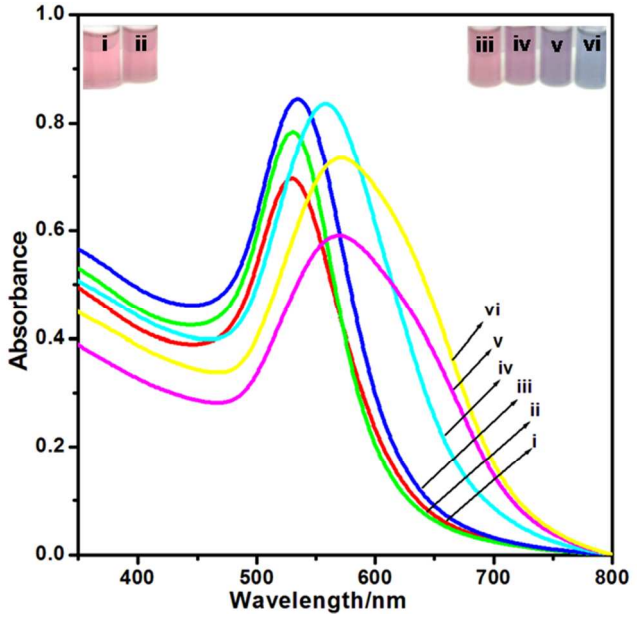


**Fig.1** UV-VIS spectra showing change in λmax of AuNPs made using constant concentration of THF-HPO (11.3 mg) and varying concentrations of 3-APTMS; (i) 0.2M, (ii) 0.3M, (iii) 0.4M, (iv) 0.5M, (v)0.6M, and (vi) 0.7M . UV-VIS spectra showing change in λmax of AuNPs made using constant concentration of THF-HPO (11.3 mg) and varying concentrations of 3-APTMS; (i) 0.2M, (ii) 0.3M, (iii) 0.4M, (iv) 0.5M, (v)0.6M, and (vi) 0.7M .

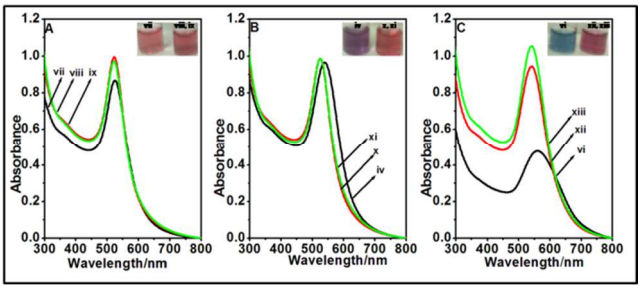


**Fig.2** UV-VIS spectra showing change in λmax of AuNPs made using increasing concentrations of 3-APTMS (A=0.25M; B=0.5M and C=0.7M) containing THF-HPO of three different concentrations [11.3 mg (black line), 33.9 mg (red line) and 56.5 mg (green line)] in each cases (vii, viii ix for A; iv, x, xi for B and vi, xii and xiii for C. Inset to A, B and C show the photograph in colour change of AuNPs before and after the addition of increased THF-HPO concentration.

enabled to justify the role of both nanogeometry and Amino functionality in chemical sensing and is discussed in later part. The results on the variation of $\lambda_{max}$ as shown in Table-1 suggest the choice of 3-APTMS concentrations corresponding to 0.2M, 0.5M and 0.7M at constant concentration of THF-HPO (11.3mg) yielding reasonable difference in size of AuNPs with $\lambda_{max}$ at 530nm, 558nm and 571nm. The corresponding TEM images are shown in Fig.3 A, B,C respectively and reveal that when the concentration of 3-APTMS increases from 0.2M to 0.7M the size of the nanoparticle increases from 10nm to 35nm.

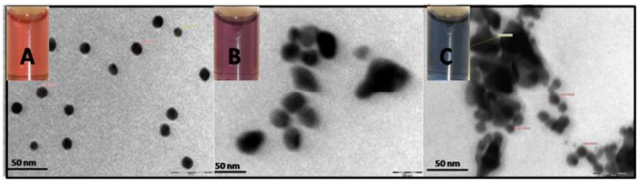


**Fig.3** TEM images of AuNPs made from increasing concentrations of 3-APTMS (A=0.25 M. B=0.5 M and C=0.7 M) containing constant concentration of THF-HPO (11.3 mg).

That means more the concentrated 3-APTMS, the larger the size of resulting AuNPs. Further nanoparticles in Fig.3A are well dispersed, symmetrical and its size is 10nm whereas the result shown in fig.3B reveals agglomeration of nanoparticles leading the nanoparticle size of 25nm. The agglomeration has further increased on increasing 3-APTMS to 0.7 M (fig.3C) resulting in nanoparticles of size 35nm. Thus data on spectrophotometry and TEM images suggest an increase in nanoparticle size with increasing 3-APTMS. Further, such increase in size is due to the agglomeration of nanoparticles with increasing 3-APTMS possibly due to combined effect of reaction products (GBL, imine derivate of GBL and 3-APTMS). These AuNPs at a fixed 3-APTMS and THF-HPO gives a single persistent colour which remains stable at room temperature for quiet a long time thus enabling it to be used for various practical purposes.

After confirming the concentration-dependent role of THF-HPO and 3-APTMS on AuNPs synthesis, we further investigated the mechanism of such process. Spectrophotometric monitoring of nanoparticle formation with time revealed the ocurrence of absorption peak at 210nm could be due to the formation of GBL from THF-HPO since the formation of GBL from THF-HPO in the presence of metal ions is known.[33] It has also been recorded that the absorbance at 210nm varies with time which suggests its formation and consumption in due course. Further to explore the role of GBL in AuNPs synthesis we synthesized GBL from THF[34] and tried nanoparticle synthesis using GBL in place of THF-HPO. The nanoparticle formation with GBL in place of THF-HPO is not of much significance, as the nanoparticles formation took comparitively long time with relatively less yield. Neverthless, GBL also triggered the AuNPs synthesis in the presence 3-APTMS. Amino capped $Au^{3+}$ ion was brought in contact with GBL (in place of THF-HPO) and was left undisturbed for 4-5 hours under two different conditions; (i) Varying 3-APTMS while keeping GBL concentration constant (fig.4A), and(ii) varying GBL (fig.4B) while keeping 3-APTMS concentration constant. Increased concentration of

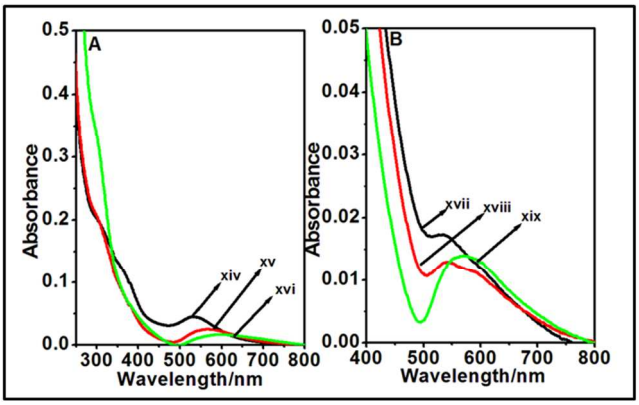


**Fig.4** UV-VIS spectra of AuNPs made from GBL and 3-APTMS showing change in λmax as a function of: (A ) variable concentrations of 3-APTMS (xvi=0.25 M, xv= 0.35 M and xvi=0.5 M) with constant concentration of GBL (40mg); (B) variable concentrations of GBL (xvii=50.0 mg, xviii= 60 mg and xix=70 mg) with constant concentration of 3-APTMS (0.25 M).

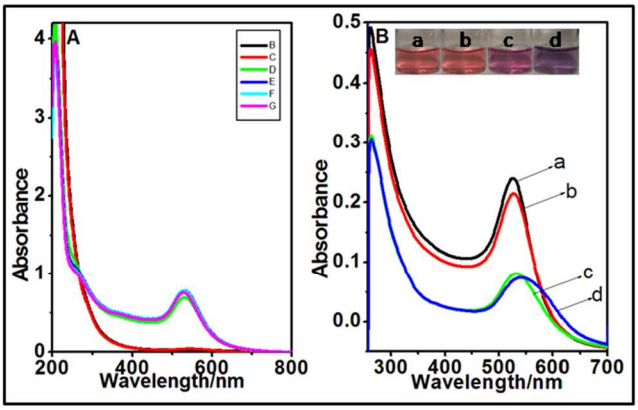


**Fig.5 (A)**Time dependent UV-VIS spectrum of AuNPs made using 3-APTMS (25mM) and THF-HPO (11.3mg) (B) Change in λmax of same AuNPs (a) on the subsequent addition of 3-APTMS; 20µl ; 50mM (b), (c) and (d).

both the reactant (GBL/3-APTMS) increased the AuNPs size as shown in table 2 and fig.4. Interestingly it was also discovered that this GBL mediated tranformation to AuNPs could be speeded up by the addition of small amount of presynthesized AuNPs.

To go further into deeper insight on the mechanistic approach, the studies on the formation of AuNPs as a function of time has been attempted as shown in fig.5A. The study reveals the appearance of peak at 210nm due to formation of GBL. Another hump at around 260nm is observed during the course of study due to Au(AuNPs)-Amine(3-APTMS) interaction. Fig. 5B gives the effect of subsequent addition of 3-APTMS (b, c and d) into AuNPs sol(a). Decrease in intensity of the peak corresponding to AuNPs with subsequent increase in 3-APTMS concentration is in sync with the decrease of peak around 260nm. $\lambda_{max}$

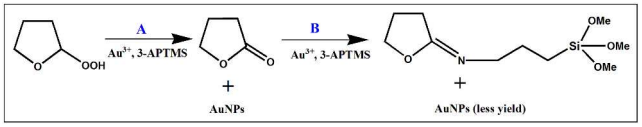


**Scheme 1** Mechanism of 3-APTMS and THF-HPO assisted synthesis of AuNPs

for AuNPs increases with increasing 3-APTMS concentration enabling the conversion of small size AuNPs into large size with subsequent reduction in the apparent number of AuNPs available for 3-APTMS interaction. Thus we conclude that with increasing size or decreasing intensity of AuNPs there is decreased Au-Amine interaction as can be seen from Fig.5B. Thus the peak around 260nm can be designated to AuNPs-Amine(3-APTMS) interaction. As can be inferred from the fig. 5A there is a synchronized decrease in intensities of absorbance of the two peaks corresponding to 210nm and 260nm, which means they are getting consumed together, that might result in imine derivative of GBL as is shown in scheme 1. It can be deduced further from the fig. 5B that the peak at around 260nm , corresponding to the AuNPs-Amine(3-APTMS) interaction , also gets decreased with increasing 3-APTMS. 3-APTMS, though is a stabilizer but its increased concentration results into an increase in AuNPs size that could be due to its consumption (via route B, discussed later). Following important conclusion can be drawn from the experimental finding discussed above; (a) an increase in size of AuNPs with increasing 3-APTMS concentration, (b) decrease in size of AuNPs with increasing THF-HPO, (c) formation of GBL during the nanoparticle synthesis. (d) formation of peak at around 260nm due to Au-Amine interaction. (e) Synchronized decrease in intensity of the peaks at 210nm (GBL) and 260nm (Au-Amine) with time and (f) Decrease in intensity of the peak at 260nm following subsequent addition of 3-APTMS accompanied with increased size of AuNPs. Based on these findings, we propose following mechanism for 3-APTMS and THF-HPO mediated synthesis of AuNPs;

Newman et al have studied in detail the reduction of $Au^{3+}$ to $Au^{0}$ involving several amine compound.[15] In our system $Au^{3+}$ in presence of THF-HPO and 3-APTMS gets reduced to form stabilized AuNPs accompanied by formation of GBL. $Au^{3+}$ reduction to $Au^{0}$ is facilitated by THF-HPO oxidation to GBL. The resulting GBL in the presence of $Au^{3+}$ and 3-APTMS may form imine derivative of GBL under optimum conditions resulting again the formation of AuNPs. Accordingly, the synthesis of AuNPs proceeds through reaction pathway A and B as shown in scheme-1. At lower 3-APTMS concentration

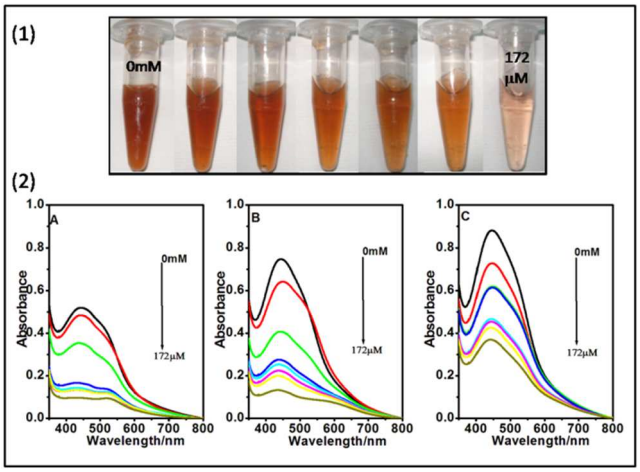


**Fig.6 (1)** A typical photograph showing effect of increasing GSH concentration on o-dianisidine-H2O2-AuNP reaction system.(2)UV-VIS spectra of o-dianisidine-H2O2-AuNPs system in the presence of varying concentration of GSH (0 mM- 172µM) for three sizes of AuNPs; (A) 10nm (B) 25nm (C) 35nm; under the optimum condition.

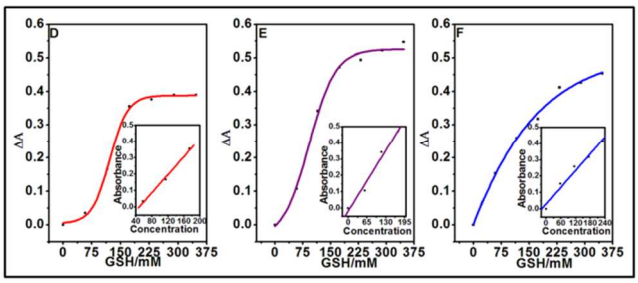


**Fig.7** Response curves of GSH detection using o-dianisidine in the presence of AuNPs of three different size (D)10nm (E) 25nm (F) 35nm. Inset shows linear calibration plot for GSH analysis

reaction mainly proceeds through pathway A and that at higher 3-APTMS pathway B comes into action as well. We have already discussed the nanoparticle synthesis using GBL and 3-APTMS as starting material and it was found that both have a kinetic role to play in imine formation. An increase in the concentration of either GBL or 3-APTMS resulted into incresaed size of AuNPs probably due to decrease in 3-APTMS content associated to route B. At higher concentration of 3-APTMS, the system also undergoes side reaction via route B, thus decreasing the 3-APTMS content and resulting nanoparticles of increased size are formed which is also evident from the TEM images of nanoparticles. Route A results in nanoparticles of smaller size, whereas route-B results in nanoparticles of higher size. This explains the higher nanogeometry with increasing 3-APTMS. The size of the synthesized AuNPs can further be manipulated by adding 3-APTMS to the synthesized AuNPs. Fig. 5B shows the change in $\lambda_{max}$ that occur as a result of subsequent additions of 3-APTMS.

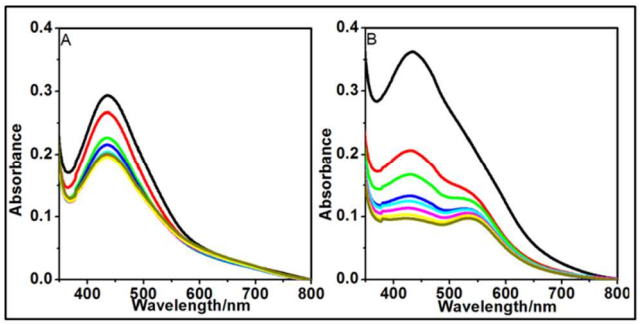


**Fig. 8** UV-VIS spectra of o-dianisidine-H2O2-AuNPs system in the presence of varying concentration of GSH (0mM-172µM). AuNPs of two size, (A=35 nm, B=10 nm) were made at constant concentration of 3-APTMS (0.7)

**Role of nanogeometry and functionality in chemical sensing**

Difference in sensory responses of nanoparticles based on their nanogeometry is much studied[19] but difference in sensory responses based on its functionality is still obscure. Here we are reporting an interesting finding on the colorimetric method for determination of GSH which is based on the competitive reaction of GSH and o-dianisidine with $H_2O_2$ in the presence of AuNPs made at three different concentrations of 3-APTMS and similar measurements were made for AuNPs of different nanogeometry but same 3-APTMS concentration. Upon the addition of AuNPs, the absorbance intensity of the o-dianisidine-$H_2O_2$ system was increased due to the intrinsic peroxidase property of 3-APTMS functionalized AuNPs, having property to catalyze H2O2-mediated oxidation of o-dianisidine.We report herein that amino functionalized AuNPs exhibit different sensory responses as a function of nanogeomtry as well as concentration of 3-APTMS used in synthesizing AuNPs. Though the peroxidase mimetic behaviour of AuNPs are known[35-36] however the nanogeometry or functionality dependent differences in peroxidase mimetic behaviour has not been much studied.

At first instance we compared three different sizes of AuNPs (10nm, 25nm and 35nm), made by using increasing concentrations of 3-APTMS, by recording the concentration dependent absorbance changes at fixed time that occur while catalyzing the oxidation of o-dianisidine in presence of $H_2O_2$ at different GSH concentration as shown in Fig.6. Fig.7 shows the relative absorbance- concentration plot for the three different sizes. The linear range and detection limit are found in the order AuNPs (35nm) > AuNPs(25nm)>AuNPs(10nm). The results demonstrate that the AuNPs made at higher 3-APTMS concentration (35 nm) shows better catalytic property/sensing ability as compared to that made at lower concentrations of the same (25 and 35 nm).

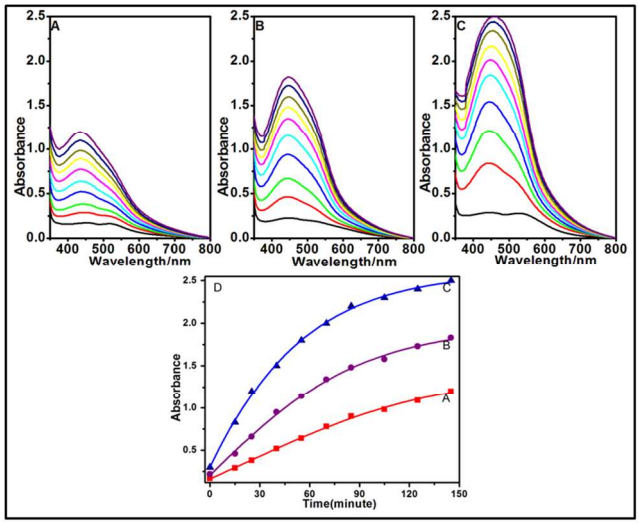


**Fig.9** Time dependent UV-VIS spectral change of o-dianisidine-H2O2 system catalyzed by AuNPs of variable size; (A) 10nm (B) 25nm and (C) 35nm. Plot-D shows the time dependent variation of absorption at 430 nm calculated from plots A, B and C respectively.

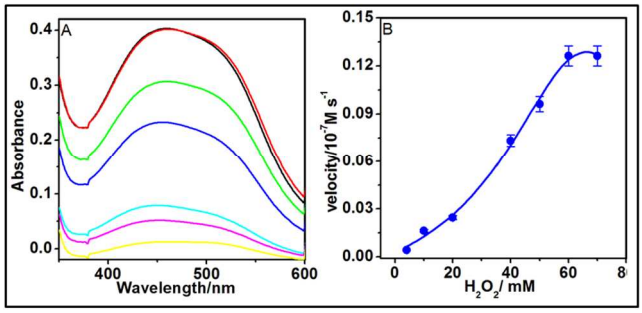


**Fig.10** Kinetic analysis of o-dianisidine-AuNPs-H2O2 system with H2O2 as substrate. H2O2 concentration is varied from to 980μM-58.9mM

It is clear from the figure-6(A, B, C) that the order is different from what it should have been on the basis of size of the nanoparticles i.e smallest catalyzing the most, which is very well known from available literature.[37-39] It is to be noted the AuNPs not only differ in size but also have different 3-APTMS concentration. Thus the possibility of amine functionality assisted catalysis might be there. Accordingly, we designed another set of experiment using AuNPs of two different size while keeping constant concentration of 3-APTMS. As we have already explained that AuNPs of different nanogeometry at same 3-APTMS concentration can be made by varying the THF-HPO content. Accordingly AuNPs of two size (35 and 25 nm) at two different concentrations of THF-HPO (11.3mg, 33.9mg ) respectively keeping constant 3-APTMS (0.7M) were synthesized. Fig.8 A and B shows the results on GSH analysis and reveals that an increase in nanogeometry causes an increase in rate of catalysis which is accordance to reported findings.[36-38] Thus the increased catalytic efficiency of AuNPs is a cumulative result of nanogeometry and functionality. It should also be noted that the role of amino functionality dominates over the nanogeometry in GSH sensing. Similar results for time dependent o-dianisidine-$H_2O_2$-AuNPs system in the absence of GSH has also been recorded as shown in Fig.9. The peroxidase-like catalytic property for the fastest system (AuNPs size = 35nm) was further investigated using steady-state kinetics. The kinetic data were obtained by varying $H_2O_2$ concentration while keeping the other substrate concentration constant as shown in Fig. 10.The kinetic analysis of o-dianisidine-AuNPs system at varying H2O2 concentrations gave Km value of 38.12mM. Although AuNPs synthesized are less competent compared to other system but it provides an opportunity for water soluble and easy to synthesize AuNPs to be used as catalyst for various practical applications.

## CONCLUSION

We observed novel findings on the controlled and rapid synthesis of AuNPs with size ranging from 10nm to 40nm based on the active participation of 3-APTMS and THF-HPO. An increase in the size of AuNPs with increse in concencentrations of 3-APTMS is recorded whereas an increase in THF-HPO concentration decreases the size of the same. Nanogeometry of as synthesized AuNPs can further be manipulated by addition of 3-APTMS even after the synthesis of the same. The flexibility in the synthesis technique allows formation of AuNPs of desired size at desired 3-APTMS and THF-HPO concentrations.The new process of AuNPs synthesis results into the conversion of THF-HPO to GBL which itself participates in nanoparticle formation under optimum concentration and forms imine derivative of GBL with 3-APTMS. The as synthesized amine functionalized AuNPs also displays peroxidase mimetic behaviour and have an additional advantage as amine functionality assists the AuNPs in its catalyzing/sensing ability. The nanoparticles synthesized differ from other nanoparticles in its catalyzing ability that increases with increasing size, in condition where both nanogeometry and functionality varies, which is attributed to the combined effect of nanogeometry and functionality. Although, when the effect of nanogeometry is studied alone by keeping amine functionality constant it shows the conventional behaviour towards catalysis. Thus the synthesized AuNPs with tunable functionality and nanogeometry may be used for various applications in future.

ACKNOWLEDGMENT

The authors are thankful to University Grants Commission (UGC) for providing financial support to carry out this work. We also thank to SAIF (AIIMS) New Delhi for providing electron microscopy facilities.

ABBREVIATIONS

3-APTMS, 3-Aminopropyltrimethoxysilane; 3-GPTMS, 3-Glycidoxypropyltrimethoxysilane; AuNPs, Gold Nanoparticles;, AgNPs, Silver Nanoparticles; PdNPs, Palladium Nanoparticles; THF-HPO, Tetrahydrofuran hydroperoxide.

.

## Notes and references

[a] *Address, Department of Chemistry, Indian Institute of Technology (BHU), Varanasi-221005, India,* pcpandey.apc@iitbhu.ac.in

1. M. C. Daniel and D. Astruc, *Chem. Rev*. 2004, **104**, 293.
2. H. Haick, *Phys. D: Appl. Phys* 2007, **40**, 7173.
3. M. Zayats, R. Baron, I. Popov and I. Willner, *Nano Lett.* 2005, **5**, 21
4. S. H. Radwan, H. M. E. Azzazy, *Expert Rev. Mol. Diagn*. 2009, **9**, 511.
5. S. D. Evans, S. R. Johnson, Y. L. Cheng and T. Shen, *J. Mater. Chem.* 2000, **10**, 183
6. H. L. Zhang, S. D. Evans, J. R. Henderson, R. E. Miles and T. Shen, *Nanotechnology* 2002, **13**, 439.
7. W. Jeong, M. J. Kim, K. Rhee,mputational study of particle size effects on selective binding of nanoparticles in arterial stenosis.2013, 43,417-424.
8. F. P. Zamborini, M. C. Leopold, J. F. Hicks, P. J. Kulesza, M. A. Malik and R. W. Murray, *J. Am. Chem. Soc.* 2002, **124**, 8958-8964.
9. C. Xu, K. Xu, H. Gu, X. Zhong, Z. Guo, R. Zheng, X. Zhang and B. Xu, *J. Am. Chem. Soc.* 2004, **126**, 3392 – 3393
10. T. Mirzabekov, H. Kontos, M. Farzan, W. Marasco, and J. Sodroski, *Nat. Biotechnol*. 2000, **18**, 649 – 654
11. S. Jain, G. D. Hirst, J. M. O'sullivan, *The British journal of radiology*. 2012,**85**,101–113
12. Daniel V. Leff, Lutz Brandt and James R. Heath*, *Langmuir,* 1996, **12**, 4723-4730
13. X. Liu, M. Atwater, J. Wang, Q. Dai, J. Zou, J. P. Brennan and Q. Huo, *J Nanosci Nanotechnol*. 2007 Sep, **7(9)**, 3126-33
14. S. K.Bhargava, J. M. Booth, S. Agrawal, P. Coloe and G. Kar, *Langmuir,* 2005, **21**, 5949.
15. M. Aslam, L. Fu, M. Su, K.Vijayamohanan and V. P. Dravid, *J. Mater. Chem*. 2004, **14**, 1795.
16. M. Aslam, L. Fu, M. Su, K.Vijayamohanan and V. P. Dravid, *J. Mater. Chem*. 2004, **14**, 1795.
17. J. D. Newmann and G. J. Blanchard, *Langmuir*, 2006 **Jun 20;22(13)**, 5882-7.
18. P. C. Pandey, S.Upadhyay and H. C.Pathak, *Electroanalysis* 1999, **11**, 59–64
19. H. Zhu, Z. Pan, E.W. Hagaman, C. Liang, S.H. Overbury and S.Dai, *Jornal of colloid and interface science*, 2005, **287**, 360-365.
20. P. C. Pandey, S. Upadhyay, I. Tiwari and Sharma S, *Electroanalysis*, 2001,**13**, 1519
21. P. C. Pandey and D. S. Chauhan, *Analyst*. 2012, **137(2)**, 376-85
22. Pandey, P. C. A process for the organic hydroperoxide-mediated synthesis of noble metal nanoparticles, bimetallic nanosol and prussian blue nanoparticles therefrom. 2153/DEL/2013
23. Y. Ma, Z. Zhang, C. Ren, G. Liu and X. Chen, *Analyst*, 2012, **137**, 485–489
24. Zheng. Ai-Xian, Cong. Zhong-Xiao, Wang. Jin-Ru, N. JuanLi, N. Huang-HaoYang, Guo-NanChen, *Biosensors andBioelectronics* ,2013, **49,** 519–524
25. R. Hong, G. Han, J. M. Fernandez, B. J. Kim, N. S. Forbes, V. M. Rotello, *J. Am. Chem. Soc.* 2006, **128(4)**, 1078-9
26. G. Schmid, R. Pfeil, R. Boese, F. Bandermann, S. Meyer, G. H. Calis and J. W. A. Van der Velden. *Chem. Ber*., 1981, **114**, 3634.
27. P. C. Pandey, A. Pandey, G. Pandey, *J. Nanosci. Nanotechnol*. In press
28. J. V. Yun, Li. Baoxin and Rui Cao, Positively-charged gold nanoparticles as peroxidiase mimic and their application in hydrogen peroxide and glucose detection.
29. P. R. Selvakannan, S. Mandal, S. Phadtare, A. Gole, R. Pasricha, S. D. Adyanthaya and M. J. Sastry, *Colloid Interface Sci.* 2004, **269**, 97.
30. S. K. Bhargava, J. M. Booth, S. Agrawal, P. Coloe and G. Kar, *Langmuir*, 2005, **21**, 5949-5956.
31. H. Rein and R. Criegee, *Angew. Chem*, 1950, **62**,120
32. M. Aslam, L. Fu, M. Su, K.Vijayamohanan, V. P. Dravid, *J. Mater. Chem.* 2004, **14**, 1795.
33. S. Murai, N. Sonoda and S.Tsutsumi, *J-STAGE*. 1962, **36**, 527-530.
34. M. Leonid and B.Shmuel, *Tetrahedron,* 2000, **56** ,1905–1910.
35. S. H. Chen, R.Yuan, Y. Q.Chai, L. Xu, N.Wang, X. N. Li, and L. Y. Zhang, *Electroanalysis* , 2006, **18**, 471.
36. Y. Y. Wang, X. J. Chen, J. J. Zhu, *Electrochem. Commun.* 2009,**11**, 323-326.
37. M. Haruta, *Catal. Today* 1997, **36**, 153-166.
38. M. Haruta, *J. New Mater. Electrochem. Syst.* 2004, **7**, 163-172.
39. B. Hvolbaek, T. V. W. Janssens, B. S. Clausen, H. Falsig, C. H. Christensen and J. K. Norskov, *Nano Today,* 2007, **2**, 14-18.

**Table1** 3-APTMS and THF-HPO mediated synthesis of AuNPs showing change in λmax as a function of reactants concentrations.

| Sample No. | 3-APTMS | THF-HPO | λmax |
|---|---|---|---|
| i. | 0.2M | 11.3mg | 526nm |
| ii. | 0.3M | 11.3mg | 530nm |
| iii. | 0.4M | 11.3mg | 532nm |
| iv. | 0.5M | 11.3mg | 553nm |
| v. | 0.6M | 11.3mg | 565nm |
| vi. | 0.7M | 11.3mg | 569nm |
| vii. | 0.25M | 11.3mg | 523nm |
| viii. | 0.25M | 33.9mg | 519nm |
| ix. | 0.25M | 56.5mg | 519nm |
| x. | 0.5M | 33.9mg | 524nm |
| xi. | 0.5M | 56.5mg | 524nm |
| xii. | 0.7M | 33.9mg | 536nm |
| xiii. | 0.7M | 56.5mg | 536nm |

**Table 2** Effect of GBL on 3-APTMS-mediated synthesis of AuNPs.

| Sample No. | 3-APTMS | GBL | λmax |
|---|---|---|---|
| xiv | 0.25M | 40mg | 531nm |
| xv | 0.35M | 40mg | 558nm |
| xvi | 0.50M | 40mg | 579nm |
| xvii | 0.25M | 50mg | 537nm |
| xviii | 0.25M | 60mg | 545nm |
| xix | 0.25M | 70mg | 571nm |